PHYSICAL REVIEW B VOLUME 9, NUMBER 4 15 FEBRUARY 1974

Study of localized levels. II. The meaning of temperature-induced changes in activation on energies for electrical conduction

F. W. Schmidlin
Xerox Research Laboratories, Rochester, New York 14644

G. G. Roberts
New University of Ulster, Coleraine, Northern Ireland

(Received 3 January 1972; revised manuscript received 27 August 1973)

It is shown that the dominant-level approximation is a generally useful method for interpreting temperature-induced changes in Ohmic activation energy. Particular emphasis is placed on the situation where a change occurs due to a reversal of the inequality between the contributed and nonextrinsic carrier concentrations. All the prime causes for a temperature-induced change in activation energy are considered and the temperature at which a change occurs is used to establish additional relationships between the dominant-state densities. A graphical means of computing the Fermi energy and locating localized-state densities is also described. The analysis is applied to recent experimental results on gallium arsenide, silicon, and phthalocyanine and old results on germanium. The results show that impurity levels previously located via interpretation of activation energies for electric conduction are often incorrect and should be relocated, using the rules and procedures presented in this paper.

I. INTRODUCTION

In a recent paper, hereafter referred to as I, Roberts and Schmidlin[1] solved the statistical problem for a semiconductor in sufficient generality to delineate all possible interpretations of a "simple activation energy" (i.e., a constant slope in a plot of $\log_{10}$ current versus reciprocal temperature). In physical terms one of the requirements for a simple activation energy to be manifest in electrical conduction is that specific energy levels must contribute overwhelmingly to partition functions of the electrons and holes. At each temperature there must be only one such dominant level for each carrier. However, very often a $\log_{10} J$ vs $1/T$ plot can be broken into a number of distinctly separate straight-line segments. If we assume that any weak temperature dependence contributed by mobility or state-density variations is negligible or removable by multiplying J by T to the appropriate power, then well-defined activation energies can be identified in different temperature regions. Of course, each temperature interval in which a simple activation energy is observable can be analyzed using the scheme presented in I. However, the transition temperature itself, defined by the intersection of neighboring extrapolated linear segments in the activation energy plot, is an additional bit of information which can be useful to establish additional relations between dominant-state densities. It is the establishment of these relations, together with guidelines or rules for interpreting the changes in Ohmic activation energy directly, which is the purpose of this paper. We show that under certain favorable circumstances all dominant-state densities can be determined. We also point out additional qualitative signals which warn against some possible interpretations attributed ordinarily to activation energies. For example, it is shown that the activation energy prior to a decrease of activation energy as the temperature increases is never an ionization energy. This has not been fully appreciated in the past and has led to incorrect locations for localized levels in a large number of materials including germanium, silicon, and gallium arsenide.

II. SUMMARY OF PAPER I

In general, both Ohmic and space-charge-limited (SCL) currents are thermally activated, their respective activation energies being contained in the quantities n_c and θ_n in the following equations:

$$J_\Omega = n_c e \mu_0 (V/L), \tag{1}$$

$$J_{sc} = \tfrac{9}{8}\, \theta_n \epsilon \mu_0 (V^2/L^3). \tag{2}$$

In these equations V is the voltage across a sample thickness L; μ_0 is the microscopic mobility; e is the electronic charge; n_c is the density of free carriers; ϵ is the permittivity; and θ_n is the fraction of total carriers (all electrons above the Fermi level) which are free.

It is shown in I that a requirement to observe a simple activation energy is either

$$(N_d - N_a)^2 \gg 4Q_e Q_p \quad \text{(extrinsic situation)}$$

or (3)

$$(N_d - N_a)^2 \ll 4Q_e Q_p \quad \text{(nonextrinsic situation)},$$

where N_d is the concentration of donors above the Fermi energy, N_a is the concentration of acceptors below the Fermi energy, and

$$Q_e \equiv N_c e^{-\epsilon_c/kT} + \sum_i N_i e^{-\epsilon_i/kT},$$
$$Q_p \equiv N_v e^{-\epsilon_v/kT} + \sum_j N_j e^{-\epsilon_j/kT} \quad (4)$$

are the partition functions for electrons and holes, respectively. As indicated in Fig. 1, the energies in Eq. (4) are measured relative to a reference (ϕ) which may be taken anywhere. Visualization of the relative sizes of the terms in the partition function is facilitated, however, by choosing it at or near the anticipated Fermi energy. A graphical solution in which ϕ is taken at the Fermi energy is described later. A second condition which must be satisfied in order to observe a simple activation energy is that single terms in Q_e and Q_p must dominate the statistics. As in I these dominant levels are labeled with subscripts m and q, respectively.

If we exclude the special case when the Fermi level happens to fall within a few kT of a relatively concentrated level, then Maxwell-Boltzmann statistics are a good approximation for the distribution of carriers and we may write

$$(N_d - N_a) = XQ_e - (Q_p/X), \quad (5)$$

where $X = e^{(\mu-\phi)/kT}$ as in I. Any level close enough to the Fermi energy to invalidate the Boltzmann approximation to the Fermi function must be excluded from Eq. (5) and dealt with explicitly. For example, suppose a level E^*, of density N^* is dubiously close to the Fermi energy. In this case, ϕ can be conveniently placed at E^* and Eq. (5) becomes

$$N^* + N_d - N_a = XQ_e + N^*/(1+X^{-1}) - Q_p/X, \quad (6)$$

where $X \equiv e^{(\mu-E^*)/kT}$. Note that the dubious level has been sorted out of Q_e and Q_p and expressed explicitly in terms of the Fermi function. The number of electrons which it can contribute has also been made explicit on the left-hand side of Eq. (6). This implies $N_d - N_a$, defined in I as the "contributed electron concentration," must be counted as if the Fermi energy lies above the questionable level. Accordingly, $N_d - N_a$ automatically increases by N^* as the Fermi energy drops below E^*. Thus,

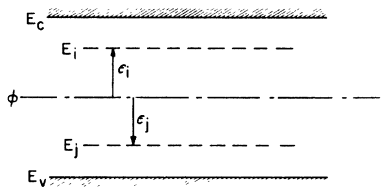

FIG. 1. Schematic energy-level diagram for a material showing the arbitrary reference level ϕ and localized levels E_i and E_j.

a localized level always behaves as if it were a donor as it ionizes regardless of its inherent charge state. It may be seen that this is a consequence of how the contributed electron concentration ($N_d - N_a$) is defined. It should be noted that such a definition is self-consistent and represents the only property of donors and acceptors manifest in statistical mechanics. The nonextrinsic carrier concentration is defined as $n_m \equiv (Q_e Q_p)^{1/2} = p_q$. It can be shown from Eq. (6) that the terms involving N^* can be dropped whenever either $N^* \ll N_d - N_a$ or $N^* \ll (Q_e Q_p)^{1/2}$. Physically this means the number of carriers involved with changes in the population of N^* would be small compared to the contributed or nonextrinsic concentration already present.

With the terms involving N^* omitted, Eq. (6) was solved in I for all cases in which a simple activation energy can be observed; namely, when expression (3) holds and single terms in the partition functions, corresponding to our dominant levels E_m and E_q, are much larger than the rest. The resulting expressions for the Fermi energy are

$$\mu = E_m + kT \ln[(N_d - N_a)/N_m] \quad (7)$$

for the extrinsic case, and

$$\mu = \tfrac{1}{2}(E_m + E_q) + \tfrac{1}{2}kT \ln(N_q/N_m) \quad (8)$$

for the nonextrinsic case. These expressions show that the Fermi energy always moves linearly with temperature as long as any pair of levels dominate the statistics. The uniqueness of this result appears not to have been fully appreciated in the past.

The population of the transport band, n_c (or p_v), and the dominant levels, n_m and p_q, lead to the following expressions for the mobile carrier concentration and θ factors, for the only cases in which a simple activation energy can be observed.

(*i*) *Extrinsic case.*

$$n_c = \frac{(N_d - N_a)N_c}{N_m} e^{(E_m - E_c)/kT}, \quad (9)$$

$$\theta_n = (N_c/N_m) e^{(E_m - E_c)/kT}. \quad (10)$$

(*ii*) *Nonextrinsic case.*

$$n_c = N_c \left(\frac{N_q}{N_m}\right)^{1/2} \exp\left(\frac{(E_m - E_c) - \tfrac{1}{2}(E_m - E_q)}{kT}\right), \quad (11)$$

$$\theta_n = (N_c/N_m) e^{(E_m - E_c)/kT}. \quad (12)$$

The most interesting result in this group is to be found in Eq. (11). We see that, for an n-type material, if the excess donor concentration is small in comparison with the concentration of electrons excited from the dominant hole level to the dominant electron level, then the Fermi energy is located between the two dominant levels in such a way as to make the concentration of electrons in

the dominant electron level equal to the concentration of holes in the dominant hole level. This is what is termed the nonextrinsic situation. It is very similar to the familiar intrinsic situation and reduces to the latter when both dominant levels are the transport bands.

Equations (9)–(12) lead to the following theorem: *The existence of different (or identical) activation energies for Ohmic and* SCL *conduction is both a necessary and a sufficient condition for Ohmic conduction to be nonextrinsic (or extrinsic).* Roberts and Schmidlin[1] exemplify this theorem by data obtained on several inorganic signal-crystal semiconductors. Their data on GaP and HgS in particular showed the first experimental characterization of the bounding sides of the Lampert triangle[2] in a single material. The theorem has also been used recently to interpret results on CdTe[3] and stilbene.[4] Further examples are described in Sec. V of this paper.

Now it is clear that a change in the activation energy for Ohmic conduction can occur whenever a new term in the electron- and hole-partition functions becomes dominant as the temperature changes. It is also clear that a similar change can occur if the Fermi energy crosses a sufficiently dense level to change the relationship between the contributed and nonextrinsic carrier concentrations. Whenever changes in the activation energy with temperature can be observed, the change in the activation energy and the temperaure at which it occurs provides valuable additional information on the energy and state density of the localized levels in a material. The purpose of this paper is to delineate the kinds of temperature-induced transitions which can occur and the nature of the information they provide.

III. GRAPHICAL SOLUTION

A simple method of solving the statistics problem graphically is described in this section. It is shown to be a valuable means by which to locate the position of the Fermi energy, to identify dominant-state densities and follow their changes with temperature.

The energy levels in Eq. (4) are measured relative to an arbitrary reference level ϕ. If ϕ is chosen to be the Fermi energy then the number of electrons in a state with density N_i may be written

$$n_i = N_i e^{-\epsilon_i/kT}.$$

Therefore

$$\log_{10} n_i = \log_{10} N_i - 0.434(\epsilon_i/kT). \tag{13a}$$

Similarly,

$$\log_{10} p_j = \log_{10} N_j - 0.434\epsilon_j/kT. \tag{13b}$$

Plotted in the schematic diagram in Fig. 2 is

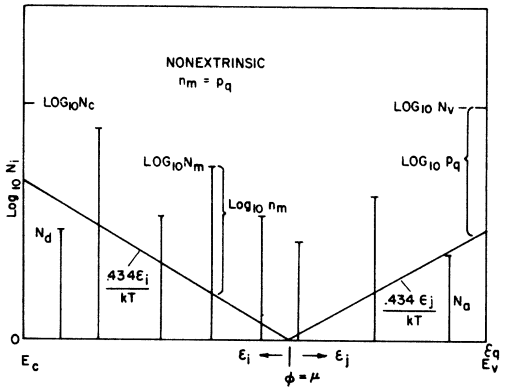

FIG. 2. Schematic energy-level diagram for a material showing $\log_{10} N_i$ and the function $0.434\epsilon_i/kT$. The extension of any state above the V gives the population of that state. The V is located assuming a nonextrinsic semiconductor.

$\log_{10} N_i$ for some arbitrary set of discrete localized levels, together with the effective band densities N_c and N_v. Continuous distributions of localized levels can be similarly replaced by equivalent discrete densities. N_d and N_a are assumed to be shallow donors and acceptors, while the other levels are assumed to be deep traps. When the latter fall below the Fermi energy they are sometimes called deep donors. Also in Fig. 2 a "V" is constructed with sides having a slope of $\pm 0.434/kT$ and with an apex that lies somewhere on the abscissa (energy axis). The objective is to slide this V along the energy axis until it falls at the Fermi energy. When the apex of the V is at the Fermi energy, the vertical extension of the states densities above the left-hand side of the V becomes the population of those states with electrons, while the vertical extension of the state densities above the right-hand side of the V becomes the population of those states with holes. Thus, one knows that the apex is properly located at the Fermi energy when either of two conditions is satisfied: (i) the total number of electrons equals the total number of holes, which is the nonextrinsic condition; (ii) the total number of electrons (or holes) equals $(N_d - N_a)$ (or $N_a - N_d$), which is the extrinsic condition. In general, it is always possible to slide the "V" so that the nonextrinsic condition is satisfied, and the solution for this case is unique. To be convinced of the uniqueness of this solution and to appreciate the ease with which it can be found, we suggest constructing your own slide rule by making the V (for the temperature of interest) on a transparent overlay and sliding the apex along the energy axis until the total number of states above the left-hand side of the V equals the total number of states above the right-hand side of the V. Since the states are plotted on

a $\log_{10}$ scale, it is generally enough to focus on the two states which have the longest extensions above the V. These are our dominant levels. The sum total of all the other occupied states ($\sum 10^{\log_{10} n_i}$, not the sum of the logarithms) is often small compared to occupation of the dominant levels. Indeed, this is a condition which must also be satisfied to observe a simple activation energy. Consequently, when a simple activation energy is measured at a particular temperature, it becomes a very simple procedure for finding the location of the Fermi energy by the procedure described above.

The only possible failure with the above solution for the nonextrinsic condition is that the n_m (or p_q) so found turns out to be smaller than $N_d - N_a$ (or $N_a - N_d$), in which case the material is really extrinsic. Of course, this is easily checked if N_d and N_a are known. The reader may readily verify that $\log_{10}(N_d - N_a) \doteq \log_{10} N_d$ is less than $\log_{10} n_m$ for the case shown in Fig. 2.

To find the Fermi energy in the extrinsic case, one must slide the V until the longest extension of some state density on the left- (right-) hand side of the V equals $N_d - N_a$ (or $N_a - N_d$). This case is illustrated in Fig. 3. Note that this solution is also unique once $N_d - N_a$ is known.

To locate the Fermi energy unambiguously, it is clearly very important to know $N_d - N_a$, or know whether the extrinsic or nonextrinsic condition applies. Such is the importance of knowing the activation energies in both the Ohmic and the space-charge-limited domains. Alternatively, it is enough to know the activation energy for Ohmic conduction if it is available over an extended temperature range and certain changes in the activation energy with temperature are observed. The procedure for interpreting changes in activation energy for Ohmic conduction with temperature is the central purpose of this paper. The graphical procedure for locating the Fermi energy at a particular temperature prepares the way for visualizing the theoretical developments in the next section.

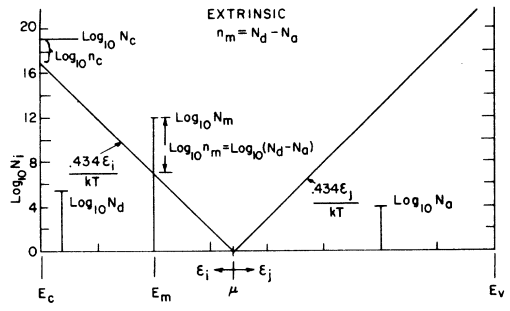

FIG. 3. Graphical analysis of the population of states in an extrinsic semiconductor.

The objective of Sec. IV is to develop rules whereby the Fermi energy can be followed and state densities can be deduced from measurements of the activation energy as a function of temperature.

Examples of this reverse procedure for finding densities and locations of the dominant levels from experimental conductivity data are described in Sec. V.

IV. THEORETICAL ANALYSIS

Barring any chemical or physical changes which create new electronic quantum states in a material, the principal cause for any temperature-induced change in activation energy is a repopulation of states, with an attendant displacement of Fermi energy. Therefore, the problem of interpreting changes in activation energy with temperature is tantamount to following the motion of the Fermi energy with temperature. At temperatures intermediate between the simple activation-energy regions, the motion of the Fermi energy becomes more complex and requires numerical analysis. Our immediate objective is to establish connections between "neighboring" simple activation-energy regions from which one can deduce how the Fermi energy must have moved during the intermediate temperature changes. By "neighboring" we mean simple activation-energy regions which are not separated by extended temperature intervals in which the dominant-level approximation obviously does not apply. A criterion for "neighboring" is a reasonably abrupt change of activation energy whose specific shape is consistent with the deduced cause for the change. For example, if a particular transition is evidently due to the Fermi energy crossing a dominant level, then it should be possible to account for the detailed shape of the transition by redoing the statistics with the Fermi function used for the population of this one level. We focus attention on neighboring simple activation-energy regions because they represent the only situation for which a transition can be attributed to a single prime cause, such as transfer of dominance between one level and another or change in the relative sizes of the contributed and nonextrinsic carrier concentrations. Only then is it possible to arrive at a well-defined relationship for the connection between the two regions. More complex transitions then can be analyzed in terms of multiple prime causes occurring simultaneously or in rapid sequence. We show how to analyze these more complex cases by examples later.

In this section we now formulate the relationships that hold when a transition between simple activation energies is due to various prime causes and

then we discuss the kind of experimental evidence which can distinguish which relationship is applicable.

A. Prime causes for temperature-induced changes in activation energies

There are three causes for a transition.

(i) A transition occurs when the two largest terms in a partition function become equal. An example of this type of transition is illustrated in Fig. 4. Note that as the temperature increases above T_1 the "V" becomes flatter and the apex (Fermi energy) moves toward the smaller dominant state density N_{q1}. Note also that the hole population of a shallower but more dense level at E_{q2} increases as T increases, and at some temperature T_{12} the population of E_{q2} becomes equal to the population of E_{q1}. At still higher temperatures, the population of E_{q2} forever remains greater than the population of E_{q1}. We say that E_{q1} has transferred its dominant role in the statistics to E_{q2} at the transition temperature T_{12}. Since dominance was transferred from one level to a shallower one of the same polarity, we call this a nonextrinsic to nonextrinsic transition. An interesting and important property of the case illustrated in Fig. 4 is that a very low state density ($< 10^7$) is capable of dominating the statistics. However, it is always necessary that the number of such states must exceed the number of mobile majority carriers. This fact is the basis of a useful rule stated later [Rule (vi)]. We obtain a relationship between the concentrations of the two levels by equating the two dominant terms in the partition function at the transition temperature T_{12} (defined by the intersection of extrapolated linear segments in a $\log_{10}J$-vs-$1/T$ plot). Thus for holes

$$N_{q2} = N_{q1}\, e^{(E_{q1}-E_{q2})/kT_{12}}, \tag{14}$$

where E_{q1} and N_{q1} describe the hole level farther from the valence band. Continuing this process we can link up the concentrations for a wide spectrum of dominant levels restricted only by the temperature range over which measurements are feasible. The equivalent relation between electron levels obviously applies when the two largest levels in the electron partition function become equal. An example of this case is illustrated in Fig. 5 at T_{12}. For electrons the sign in the exponential should be reversed if the convention is adopted of assigning the lower index number to the dominant level further from the relevant transport band, i.e., the level which dominates in the lower-temperature region.

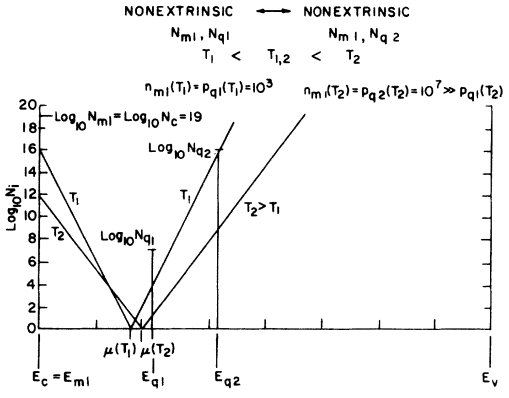

FIG. 4. Graphical analysis of the population of states in a semiconductor which undergoes a nonextrinsic to nonextrinsic transition. In order to simplify the diagram all donor or acceptor states have been excluded and the conduction band is treated as the dominant and only electron level.

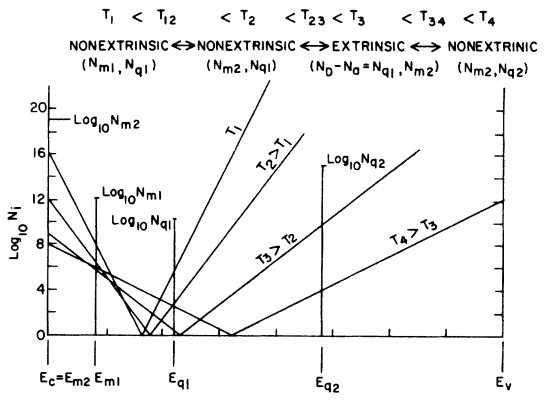

FIG. 5. Graphical analysis of the population of states in a semiconductor which undergoes a nonextrinsic to nonextrinsic transition when the two largest levels in the electron partition function becomes equal, followed by a sequence in which the conduction transforms from nonextrinsic to extrinsic to nonextrinsic again.

(ii) A transition occurs when the "majority" carrier shifts from electrons to holes or vice versa. Here "majority" means the carrier for which the concentration mobility product is the larger, although strictly speaking, a majority carrier is the one having the higher concentration. However, since we are now concerned with a shift in the activation energy for Ohmic conduction, we must include the microscopic mobilities in the relationship which holds at the transition temperature. Adding subscripts n and p to distinguish the microscopic mobilities, we obtain

$$N_q = N_m \frac{\mu_{op} N_v}{\mu_{on} N_c} \exp\left(\frac{(E_c - E_m) - (E_q - E_v)}{kT_{12}}\right). \tag{15}$$

Application of Eq. (15) is restricted to cases in which conduction is nonextrinsic both before and

after a transition. In practice, this is almost always the case, although it is possible for the majority carrier to change sign in a direct transition from an extrinsic to a nonextrinsic condition. However, this would require the unusual circumstance in which $\mu_0\theta$, the drift mobility, is very much greater for the minority carrier (prior to the transition) than for the majority carrier. Rather than construct a special relationship for this unusual circumstance we simply draw attention to the fact that is can occur.

(iii) Finally, a transition occurs when the inequality between the contributed and nonextrinsic carrier concentrations reverses. In this case we have

$$(N_{qi}N_m)^{1/2} = (N_d - N_a) \times \exp\{[(E_c - E_{qi}) - (E_c - E_m)]/2kT_{12}\} . \quad (16)$$

Here we have assumed the extrinsic case is n-type (more donors than acceptors) but the modification required if the extrinsic case is p type is straightforward. Equation (16) applies regardless of which direction the transition goes while the temperature increases. A case in which conduction transforms from nonextrinsic to extrinsic to nonextrinsic again is illustrated in Fig. 5. Note that it is important to distinguish whether the direction of the transition is nonextrinsic to extrinsic or vice versa because the minority level [E_{qi} in Eq. (16) must be different in the two directions]. If, for example, the dominant hole level is E_{qj} for some particular nonextrinsic to extrinsic transition then the dominant hole level for a subsequent transition back to a nonextrinsic condition will be $E_{q(j+1)}$ (with $E_{q(j+1)}$ being closer to the valence band than E_{qj}).

For the special case of a nonextrinsic to extrinsic transition we have the additional relation

$$(N_d - N_a) = N_{q,i} . \quad (17)$$

This relation is especially useful because it enables complete determination of all state densities when it is combined with Eqs. (16), (1), (2), and (9)–(12). Equation (17) follows from Eq. (6) and recognition of the fact that the only time the contributed or nonextrinsic carrier concentration can be altered significantly by the Fermi energy crossing a level [designated as N^* in Eq. (6)] is when the level being crossed is a dominant level at the moment of crossing. This property of the dominant levels is depicted in Figs. 4 and 5. In Fig. 4, N_{q1} yielded dominance to N_{q2} before the Fermi energy crossed it. Thus, it will never become significant again as T increases. N_{q1} in Fig. 5, on the other hand, is crossed while it is dominant and thus accounts for the appearance of the extrinsic condition.

B. Empirical identification of prime causes for a transition

Here we discuss the problem of empirically identifying which prime cause actually produces a particular transition. In doing so we shall make use of our theorem which states that a comparison of the activation energies for Ohmic and SCL conduction uniquely determines whether Ohmic conditions are extrinsic or nonextrinsic. Hence we assume this test can actually be made both before and after a transition in all that follows.

We first consider an example in which temperature is increased from $T = 0$ and conditions are nonextrinsic to start with. The first transition may go to another nonextrinsic condition or to an extrinsic condition. If the final condition is again nonextrinsic then either Eq. (14) or Eq. (16) applies. To select between these two it is necessary to first note whether the activation energy for the Ohmic region increased or decreased while going from the lower- to higher-temperature region. If it decreased then Eq. (14) applies because a decrease can only mean that the dominant level for the majority carrier has changed. If it increased, the choice remains unclear for it could mean either the majority carrier has changed sign [in which case Eq. (15) applies] or the dominant level for the minority carrier has changed [in which case Eq. (14) again applies]. To help distinguish between the latter two possibilities, the current voltage behavior at higher voltages again can be useful. Specifically, if a V^2 (SCL) behavior can be observed both before and after a transition, then it is clear that the majority carrier has not changed sign. But if SCL conduction cannot be achieved at voltages where it would normally be expected after a transition, then it is very likely that the majority carrier has changed sign. Of course, the current required may be prohibitive but this is only a practical difficulty—normally circumventable by pulse measurements. In exceptional cases, the current may actually break into a $V^{1/2}$ dependence instead of a V^2 dependence, then the contacts have definitely switched to blocking[5] and it is clear that the majority carrier has definitely switched sign. Unfortunately, this positive test for showing that the majority carrier has changed sign is possible only under very special circumstances. So, short of a Hall measurement or some equivalent means, we must generally rely on the above negative means for establishing the occurrence of a sign change for the majority carrier—the essential distinction which must be made to determine whether Eq. (14) or (15) is the applicable connecting formula. In most cases the majority carrier will not have changed. The task of selecting the applicable connecting formula if the final condition of the first transition is extrinsic is much easier. In this case

Eqs. (15) and (17) both apply and there is no other selection to make.

Subsequent to an extrinsic transition, the next transition should be back to a nonextrinsic condition with the majority carrier remaining the same sign (barring the exception mentioned earlier). This time, Eq. (16) alone applies with the dominant hole level now being closer to the valence band than the hole level which was dominant prior to the nonextrinsic to extrinsic transition. In other words, an extrinsic condition can be regarded as an intermediate condition which interrupts a normal nonextrinsic to nonextrinsic transition in which the dominant level for the minority carrier transfers from E_{qj} to $E_{q(j+1)}$. Thus, a nonextrinsic-extrinsic-nonextrinsic sequence forms a kind of closed "cycle." Since this is really the only deviant from any direct nonextrinsic to nonextrinsic transitions that can arise, any subsequent transition must be one of the types already considered. Of course, it is possible that an extrinsic condition can be the first condition observed at $T = 0$, providing the doping is appropriate. In this case, the first transition will normally be to a nonextrinsic condition. Subsequent transitions at higher temperatures will then become of the same variety as above.

The above example show how to identify the initial and final conditions of a transition and thereby select the applicable relationship from Eqs. (14)–(17). The key relationship among these equations which enables complete determination of all state densities is Eq. (17). It applies for nonextrinsic to extrinsic transitions only. Another particularly useful relation, however, is Eq. (15), i.e., the one which applies when the majority carrier changes sign. Such a transition is of exceptional value when it can be identified because it is the only one which enables unambiguous determination of a band gap from conductivity measurements.

C. Rules for interpreting temperature-induced changes in Ohmic activation energies

When the activation energies alone are of interest, we can summarize the foregoing results in the form of rules for interpreting changes in the activation energy for Ohmic conduction: In each case we refer specifically to the *change* in slope of a $\log_{10} J$-vs-$1/T$ plot as the temperature *increases*. All these rules follow directly from inspection of Eqs. (6)–(12). They may also be deduced from inspection of Figs. 4 and 5.

(i) An increase of slope is $\frac{1}{2}(E_m - E_q)$, or half the energy separation between dominant levels for the majority and minority carriers, if the initial condition is extrinsic.

(ii) An increase of slope is $\frac{1}{2}(E_{q1} - E_{q2})$, or half the energy separation between two successive dominant minority-carrier levels, if the initial condition is nonextrinsic and the majority carrier has not changed sign.

(iii) An increase of slope is $(E_q - E_v) - (E_c - E_m)$ or the difference between the depths of the dominant electron and hole levels, if the initial condition is nonextrinsic and the majority carrier has changed sign (electron to hole in the quantitative example).

(iv) A decrease of slope is $\frac{1}{2}(E_m - E_q)$, or half the energy separation between the dominat levels if the final condition is extrinsic. (E_q in this rule must be farther from the valence band than the E_q in Rule i. Also, it can never be the valence band E_v.)

(v) A decrease of slope is $\frac{1}{2}(E_{m2} - E_{m1})$, or half the energy separation between successive dominant levels for the majority carrier, if the final condition is nonextrinsic. This can only occur if the initial condition is also nonextrinsic.

(vi) A decrease in slope implies the initial condition is nonextrinsic.

The first of these rules may be recognized as a generalization of the traditional one from the early treatment of narrow-band-gap semiconductors, i.e., the higher activation energy corresponds to half the band gap because conduction is intrinsic in that region. Our rule is consistent with this but more general because it points up the fact that the final condition is nonextrinsic and that additional conditions must be satisfied to identify the final condition as intrinsic. The remaining rules are fairly self-evident but it is of interest to note that a final intrinsic condition at sufficiently high temperatures can be finally arrived at by a decrease in activation energy as well as an increase. In other words, the activation energy at various intermediate points can be greater than half the band gap as well as less than half the band gap. Rule (vi) is especially useful because it rules out the possibility that the higher activation energy in the lower temperature region is an ionization energy. This rule is exemplified in the next section where it is used to show that deep levels produced by various metals in a number of semiconductors have been incorrectly located.

V. ANALYSIS OF EXPERIMENTAL DATA

The efficacy of the interpretable scheme discussed in Secs. III and IV is now illustrated by application to other authors' data on various semiconductors.

An inverse graphical procedure for finding localized levels from resistivity versus reciprocal temperature curves is illustrated by reinterpreting early data obtained by Tyler, Newman, and Woodbury on single-crystal germanium doped with iron,[6] cobalt,[7] nickel,[8] and manganese.[9] The deep levels associated with these impurities are still cited in review articles,[10,11] but were located incorrectly.

The above error was found as the result of an effort to find examples of our rules in Sec. IV. The data on germanium proved exceptional in this respect. More recent data on silicon[12] and gallium arsenide[13] provide additional examples of Rules (iv), (v), and (vi). Data on metal-free phthalocyanine and copper phthalocyanine provide additional examples of Rules (i) and (iii).

A. Germanium

With Rule (vi) in mind, inspection of the resistivity vs $1/T$ plots of Tyler *et al.*, an example of which is reproduced in our Fig. 6, immediately shows that the low-temperature (high-resistance) region must be nonextrinsic because it is immediately followed by a lower activation-energy region as the temperature increases. Therefore, the activation energy associated with the lower-temperature region cannot be an ionization energy as previously assumed. Consequently, all the data on germanium must be reinterpreted. This is done here, first using the graphical approach and then a computer in order to make second-order adjustments to get a good fit between theory and experiment.

The band gap E_g of germanium is approximately 0.66 eV at 300 °K. If $E_g = E_{g0} - \beta T$, it may be seen that the effect of the band motion is to change the effective density of states. That is,

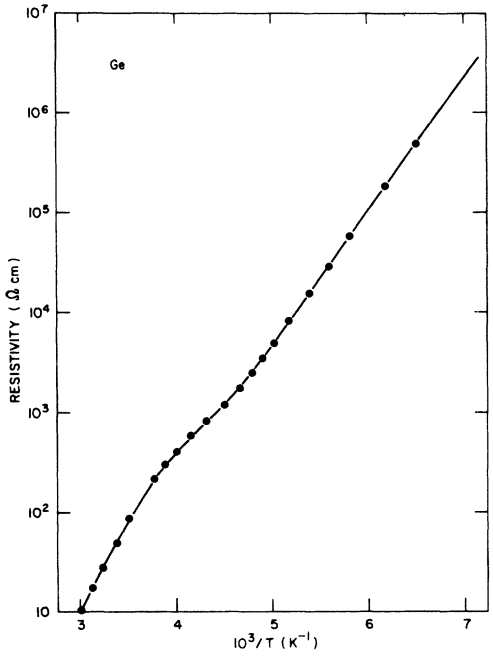

FIG. 6. Resistivity of iron-doped germanium sample "112L" as measured by Tyler *et al.* (Ref. 6) vs reciprocal temperature (points). The solid line is the computer fit obtained for parameters listed in the text.

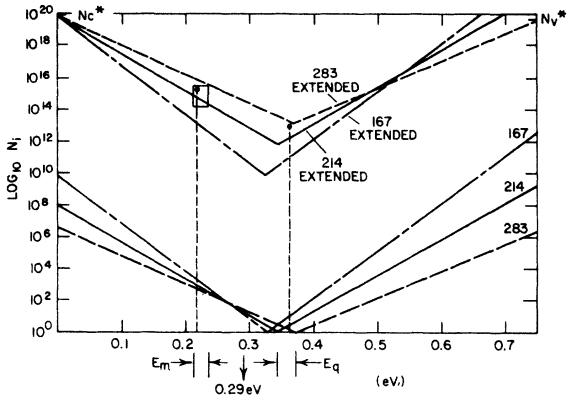

FIG. 7. Graphical analysis of the population of states on the iron-doped germanium sample labeled "112L" whose resistivity is described in Fig. 6 of the paper by Tyler *et al.* (Ref. 6).

$$N_v^* N_c^* \equiv N_v N_c e^{\beta/k} .$$

It is consistent with the data of Tyler *et al.* to put $E_g(0) = 0.74$ eV and $\beta = 0.08$ eV/300 °K. If these "excess states" are shared equally between the conduction and valence bands then, using the values of N_c and N_v quoted in Ref. 11,

$$N_c^* = 7\times10^{19}\,\mathrm{cm}^{-3}; \quad N_v^* = 4.2\times10^{19}\,\mathrm{cm}^{-3} .$$

These effective state densities separated by $E_g(0)$ provide an initial framework for plotting state densities as shown in Fig. 7. To locate within this framework the two dominant levels associated with the low-temperature nonextrinsic region identified in Fig. 6, we use the following procedure: From the microscopic mobility data on the same sample (as provided in Ref. 6, for example, 112L, n-type Fe-doped Ge) and the magnitude of the resistivity, we first compute the corresponding carrier concentration (n_c for n-type) at selected temperatures and construct the corresponding "V"'s. Three such "V"'s are constructed in Fig. 7 corresponding to 167, 214, and 283 °K. At 167 °K, the low-temperature nonextrinsic condition is still undisturbed, so we know that N_m and N_q must extend equally above this V by an amount which is larger than n_c. In other words, N_m and N_q must still extend equally above the same V after it is raised (by n_c) to pass through N_c^*. This raised V is shown dashed in Fig. 7. At 283 °K, the high-temperature intrinsic condition appears fully established. This means $n_c = p_v$ at this temperature and both n_m and p_q must be less than n_c. Thus, N_m and N_q must fall below the 283 °K "V" raised to pass through N_c^*. (Note that this raised V must also pass through N_v^*.) The two raised V's together determine a closed region inside of which both N_m and N_q must fall. It

is apparent the two temperatures should be picked as close to the transition region as possible. It is now possible to pinpoint the location of N_m and N_q more closely. At 214 °K, it appears that the first transition away from the low-temperature nonextrinsic condition has at least started. If we take this as an estimate of a first transition temperature, then we can locate the dominant level more accurately. There are two cases to consider, depending on whether the next condition is nonextrinsic or intrinsic. If the next condition is nonextrinsic, with N_m shifting dominance to the next shallower level, probably N_c, then N_m must fall very nearly on the left-hand side of the 214 °K V after it too is raised to pass through N_c. At the same time E_q must fall to the right of the apex of this "V." This restricts E_q to the fairly narrow energy interval between the Fermi energies at 214 and 283 °K. (From the information used so far E_q could be to the right of the intrinsic Fermi energy; but this is ruled out by the fact that an extrinsic condition does clearly develop for more highly Fe-doped samples.) With E_q confined between the Fermi energies at 214 and 283 °K and the requirement that E_q and E_m must be placed symmetrically about the nonextrinsic activation energy of 0.29 eV, we establish that N_m must fall within the small rectangular box shown in Fig. 7. If the next condition approached is extrinsic instead of nonextrinsic, then we can make use of Eq. (17), or $N_d - N_a = n_m = N_q$, and N_q must fall at the apex of the 214 °K V raised this time to pass through the top of N_m. After combining this with the earlier requirement that N_m and N_q must fall equally above the 167 °K V, both N_m and N_q can be very closely estimated. (It should be noted that either of the two possible locations so found are not accurate only because the transition temperature is not accurate.)

The foregoing alternative locations of N_m and N_q are nearly the same and neither can be logically ruled out. As realized later from the computer solution, this is because both transitions actually occur in rapid sequence in this sample with neither intermediate condition fully developing. The sequence which best describes the actual situation is nonextrinsic to nonextrinsic to extrinsic to intrinsic, all occurring between the 167 and 283 °K and involving the same two dominant levels. It is unfortunate that we accidentally selected this complex case to explain our inverse graphical approach. In less complex cases where the transitions are distinct (widely separated) the graphical solution pinpoints the dominant levels quite accurately. On the other hand, illustration of the procedure with this complex case demonstrates its effectiveness in blocking out bounds on allowed solutions. This proves to be an extremely helpful guide in finding a more accurate computer solution.

To locate N_m and N_q more accurately, we have used a computer to select parameters which provide the best fit to entire resistivity versus reciprocal temperature curve. The solid line shown in Fig. 6 is our computed curve for the following parameters:

$$E_c - E_v = 0.74 \text{ eV}, \quad N_c^* = 7\times10^{19} \text{ cm}^{-3},$$
$$N_v^* = 4.2\times10^{19} \text{ cm}^{-3},$$
$$E_c - E_m = 0.217 \text{ eV}, \quad N_m = 2.5\times10^{15} \text{ cm}^{-3},$$
$$E_c - E_q = 0.363 \text{ eV}, \quad N_q = 1.0\times10^{13} \text{ cm}^{-3}.$$

At no point does the computed curve differ from the experimental data (shown as points on Fig. 6) by more than 2%. The corresponding estimated accuracy in the determination of the parameters is ±0.005 eV in energy and approximately 20% in concentration.

Similar analysis of data in Ref. 6 on other Fe-doped samples resulted in almost identical values for the energies but greatly different concentrations as expected.

Careful analysis of the data for crystals of germanium doped with nickel, cobalt, and iron, both n-type and p-type, showed that in all cases a complicated set of transitions similar to those described above were responsible for the activation energy curves reported for these materials. Our computer results for the newly located energy levels introduced by Ni, Co, and Fe in germanium are summarized in Fig. 8.

Germanium crystals doped with manganese give rise to conductivity data which are quite different from those described previously for samples doped with other transition elements of the fourth row of the periodic table. For example, Fig. 9 of this paper shows the experimental data (points) for the n-type sample described in Fig. 3 of Ref. 9. We have obtained an excellent computer fit to these data (solid line) with the following parameters:

$$E_c - E_v = 0.74 \text{ eV}, \quad N_c^* = 7\times10^{19} \text{ cm}^{-3},$$
$$N_v^* = 4.2\times10^{19} \text{ cm}^{-3},$$
$$E_c - E_m = 0.21 \text{ eV}, \quad N_m = 1.8\times10^{16} \text{ cm}^{-3},$$
$$E_c - E_q = 0.575 \text{ eV}, \quad N_q = 1.8\times10^{17} \text{ cm}.$$

Woodbury and Tyler[9] interpreted the activation energies involved as ionization energies. However, we see that the kink in the activation energy curve arises due to a nonextrinsic to nonextrinsic transition identical to the one described later for GaAs.

Unfortunately, mobility data were not reported for this sample. Hence, mobility data on similarly doped samples were used to obtain the above fit. However, more accurate mobility data would not significantly alter the locations of E_q and E_m but it

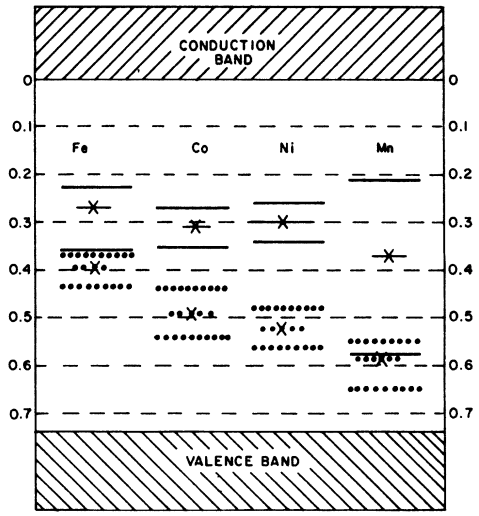

FIG. 8. Impurity levels introduced into germanium by various elements of the fourth row of the Periodic Table. The data were obtained by computer fitting experimental results reported by Tyler, Newman, and Woodbury (Refs. 6–9). The dots indicate levels calculated for p-type samples while the straight lines indicate levels calculated from n-type samples. The incorrect levels previously assigned to these impurities are shown crossed (×).

could slightly change the corresponding densities.

The data for p-type germanium doped with manganese reported in Fig. 1 of Ref. 9 (partially reproduced in our Fig. 10) provides a simple case which can be readily solved graphically. Two distinct nonextrinsic to extrinsic transitions are evident at approximately 85 and 215 °K, respectively, with the valence band dominant in both cases (zero activation energy in the extrinsic condition). Construction of the "V"'s for these two temperatures places their apexes (Fermi energies) at 0.087 and 0.20 eV from the valence band at 85 and 215 °K, respectively. Since both are transitions to the extrinsic condition, with the valence band dominant, we know that $p_v \doteq N_{a1}$ at 83 °K and $p_v \doteq N_{a2} + N_{a1}$ at 215 °K. Thus, $N_{a1} \doteq 2.7\times10^{14}$ cm^{-3} and $N_{a2} \doteq 3\times10^{14}$ cm^{-3}. A more careful computer fit, shown by the solid curve in Fig. 10, provides the following parameters:

$$E_c - E_v = 0.74 \text{ eV}, \quad N_c^* = 7\times10^{19} \text{ cm}^{-3},$$

$$N_v^* = 4.2\times10^{19} \text{ cm}^{-3},$$

$$E_{a1} - E_v = 0.08 \text{ eV}, \quad N_{a1} = 2.8\times10^{14} \text{ cm}^{-3},$$

$$E_{a2} - E_v = 0.19 \text{ eV}, \quad N_{a2} = 3\times10^{14} \text{ cm}^{-3}.$$

The excellent fit over the extended temperature region shows that no other localized levels that

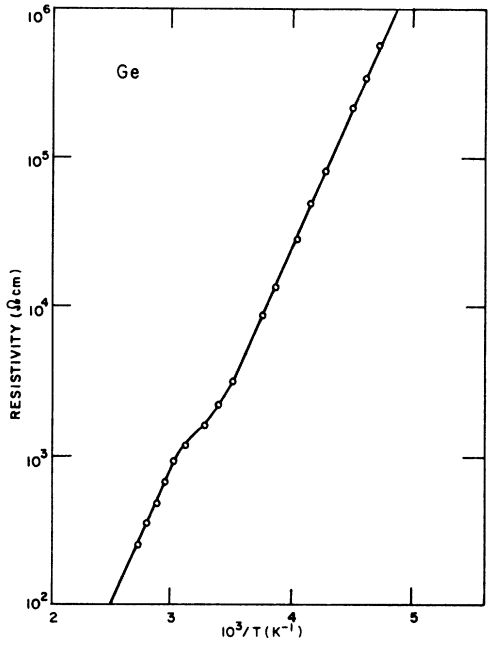

FIG. 9. Resistivity of manganese-doped n-type germanium as measured by Woodbury and Tyler (Ref. 9) vs reciprocal temperature (points). The full line is the computer fit obtained for parameters listed in the text.

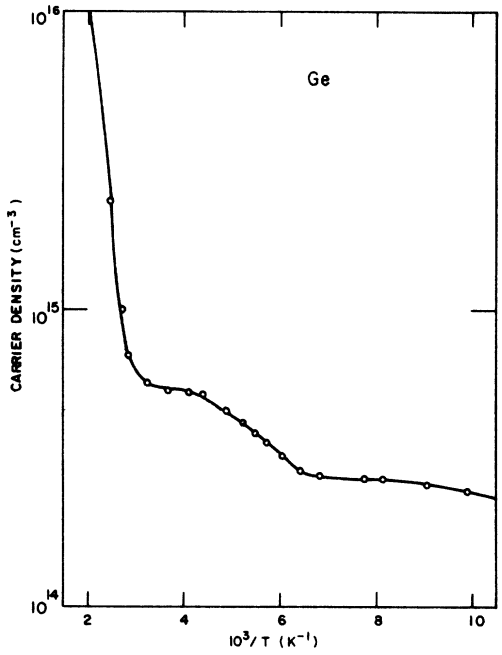

FIG. 10. Carrier density of manganese-doped p-type germanium as measured by Woodbury and Tyler (Ref. 9) vs reciprocal temperature (points). The solid line is the computer fit obtained for parameters listed in the text.

may be present in this sample can be statistically significant.

B. Silicon

Chua and Rose[12] have recently reported conductivity data for single crystals of high resistivity nickel-doped silicon. For the majority of samples, both n-type and p-type, the activation energies they observed decreased as the temperature increased. The two activation energies they obtained in each case were interpreted as acceptor-level ionization energies. We have analyzed carefully curve $N6$ in Fig. 2 of their paper. Our results are shown in Fig. 11 of this paper. The points are the experimental data of Chua and Rose while the solid line is the computer curve obtained for the following parameters:

$$E_c - E_v = 1.10 \text{ eV}, \quad N_c = N_v = 4\times10^{19} \text{ cm}^{-3},$$

$$E_c - E_m = 0.28 \text{ eV}, \quad N_m = 3\times10^{14} \text{ cm}^{-3},$$

$$E_c - E_q = 0.44 \text{ eV}, \quad N_q = 2\times10^{12} \text{ cm}^{-3}.$$

The transitions in this case are identical to those described earlier to explain the conductivity curves obtained for iron doped germanium. That is, nonextrinsic (N_m, N_q) at low temperatures, converting to extrinsic and finally, at high temperatures to intrinsic.

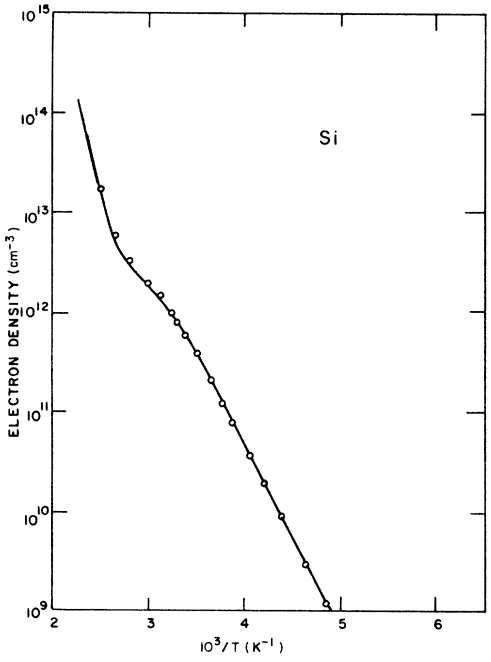

FIG. 11. Electron density obtained from Hall-effect measurements on a sample of n-type Si by Chua and Rose (Ref. 12) as a function of reciprocal temperature (points). The solid line is the computer fit obtained for parameters listed in the text.

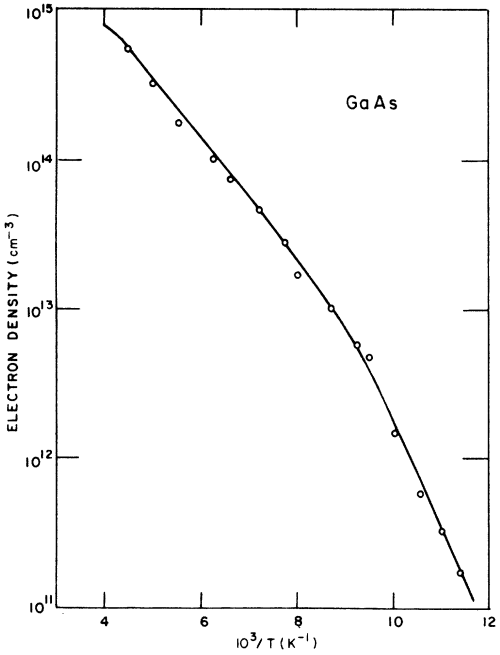

FIG. 12. Electron density obtained from Hall-effect measurements on a sample of n-type GaAs by Brehm and Pearson (Ref. 13) as a function of reciprocal temperature (points). The solid line is the computer fit obtained for parameters listed in text.

C. Gallium arsenide

Brehm and Pearson[13] have recently reported conductivity data for single crystals of epitaxially grown GaAs irradiated with electrons or x rays. For the majority of samples, both n-type and p-type, the activation energy decreases as the temperature increases. For example, curve (d) in Fig. 1 of their paper shows two clearly defined straight line sections. The activation energies observed above and below 108 K (~0.08 and ~0.13 eV, respectively) were interpreted as ionization energies of energy levels introduced by the irradiation. However, Rule (vi) in Sec. IV of this paper states that a decrease in slope implies that the initial condition is nonextrinsic. By plotting the appropriate "V" for a temperature in each of the two regions it may easily be shown using our graphical approach that a nonextrinsic-nonextrinsic transition occurs in GaAs similar to that sketched in Fig. 4. The points on the curve of electron density versus reciprocal temperature shown in Fig. 12 are the experimental data versus reciprocal temperature shown in Fig. 12 are the experimental data obtained by Brehm and Pearson[13] from Hall measurements for an n-type sample of GaAs. The solid line is our computed curve for the following parameters:

$E_c - E_v = 1.52$ eV, $N_c = N_v = 10^{18}$ cm^{-3},

$E_c - E_m = 0.10$ eV, $N_m = 3 \times 10^{13}$ cm^{-3},

$E_c - E_q = 0.15$ eV, $N_q = 1.35 \times 10^{15}$ cm^{-3}.

It is clear from these values that the transition at approximately 108 °K to a lower activation energy as the temperature is increased results from the conduction band taking over from N_m as the dominant electron level. That is, below 108 °K, the two levels controlling the position of the Fermi level are situated 0.10 and 0.15 eV from the conduction band resulting in an activation energy of 0.125 eV. Above 108 °K the average energy depth of the dominant electron and dominant hole levels is reduced to 0.075 eV.

D. Phthalocyanine

Barbe and Westgate[14] have carried out careful conductivity measurements on β-form metal-free phthalocyanine and have established the correct thickness and voltage dependences for both Ohmic and SCL currents. The activation energy for the Ohmic current through their samples changes from 0.38 eV below 363 °K to 1.05 eV above this temperature. By contrast the activation energy of the SCL current is 0.38 eV throughout the temperature range studied. The temperature induced change in the Ohmic activation energy must be interpreted via Rule (i) and thus reveals that metal-free phthalocyanine undergoes an extrinsic → nonextrinsic transition as the temperature increases through 363 °K. Following the procedure adopted in I it is possible to calculate the important state densities and their location in the energy gap. If we choose $\mu = 5$ cm^2 volt^{-1} sec^{-1} and $N_c = 10^{20}$ cm^{-3}, we find that the densities of the dominant electron and hole states are $\sim 4.10^{19}$ and $\sim 1.5 \times 10^{21}$ cm^{-3}, respectively. The latter value, which is approximately equal to the molecular density of metal-free phthalocyanine suggests that the dominant hole level is the appropriate transport band. This is consistent with the Ohmic and SCL activation energies above 363 °K (1.05 and 0.38 eV, respectively) which indicate two dominant statistical levels at $(2 \times 1.05 - 0.38) = 1.72$ eV, and 0.38 eV, from the conduction band edge. The well-established value of the band gap of this material is 1.72 eV. In contrast to the phthalocyanine results, identical low- and high-field activation energies have been reported for polycrystalline stilbene films by Gritsenko and Kurik[4] which is indicative of extrinsic conduction in this material.

Heilmeier and Harrison[15] have studied the conductivity and Hall mobility in single crystals of copper phthalocyanine in the temperature range 300–425 °K. In one of their samples the Hall mobility changed sign from negative to positive for temperatures above 100 °C. This was approximately the same temperature at which the activation energy for conductivity changed from 0.83 to 1.0 eV. The observation of a change in sign of the Hall constant together with the change in activation energy indicates that two carrier effects are present and that Rule (iii) has to be applied to the situation. Unfortunately, no SCL activation energies were measured but if we assume the most probable state of affairs, i.e., a nonextrinsic sample both before and after the transition, then we obtain $(E_q - E_v) - (E_c - E_m) = 0.17$ eV and a "band" gap, $E_c - E_v = 1.83$ eV.

VI. CONCLUSIONS

It is clear that a great deal can be learned about characteristic energies and concentrations of localized levels by examining the dependence of both Ohmic and SCL conduction on temperature over as wide a range as is experimentally feasible. We have shown in this paper that the dominant-level approximation is also a generally useful method for interpreting temperature induced changes in Ohmic activation energy. All of the six rules formulated in Sec. IV for interpreting transition temperatures have been illustrated in the experimental part of this paper.

An important aspect of the paper has involved a method by which the statistics problem for a semiconductor may be solved graphically. We have shown that, provided the experimental information is sufficiently complete to enable one to calculate the carrier concentrations in the solid, by constructing "V" at appropriate temperatures, one can obtain a good estimate of the locations and concentrations of the dominant levels in the solid.

One of the conclusions was that a decrease in the activation energy as the temperature is increased, means the initial lower temperature activation energy is *not* an ionization energy. This fact has not been fully appreciated in the past and has led to our reinterpreting experimental data on the commercially important semiconductors germanium, silicon, and gallium arsenide. Indeed there are numerous instances in the literature where authors have incorrectly interpreted their conductivity data. Five recent examples in what is certainly an incomplete list are to be found in published results on gallium sulfide,[16] tin dioxide,[17] silicon arsenide,[18] and gallium arsenide,[19] and silicon.[20]

ACKNOWLEDGMENTS

The authors wish to thank J. I. Polanco for his kind assistance with the computer programming.

[1]G. G. Roberts and F. W. Schmidlin, Phys. Rev. 180, 785 (1969).
[2]M. A. Lampert, Phys. Rev. 103, 1648 (1956).
[3]P. Mackus, A. Sakalos, A. Smilya, and J. Viscakas, Phys. Status Solidi A 2, 171 (1970).
[4]N. I. Gritsenko and M. V. Kurik, Phys. Status Solidi A 3, K57 (1970).
[5]F. W. Schmidlin, G. G. Roberts, and A. I. Lakatos, Appl. Phys. Lett. 13, 353 (1968).
[6]W. W. Tyler and H. H. Woodbury, Phys. Rev. 96, 874 (1954).
[7]W. W. Tyler, R. Newman, and H. H. Woodbury, Phys. Rev. 97, 669 (1955).
[8]W. W. Tyler, R. Newman, and H. H. Woodbury, Phys. Rev. 98, 461 (1955).
[9]H. H. Woodbury and W. W. Tyler, Phys. Rev. 100, 659 (1955).
[10]E. M. Conwell, Proc. I. R. E. 46, 1293 (1958).
[11]S. M. Sze, *Physics of Semiconductor Devices* (Wiley, New York, 1969), p. 30.
[12]W. B. Chua and K. Rose, J. Appl. Phys. 41, 2644 (1970).
[13]G. E. Brehm and G. L. Pearson, J. Appl. Phys. 43, 568 (1972).
[14]D. F. Barbe and C. R. Westgate, Solid State Commun. 7, 563 (1969).
[15]G. H. Heilmeier and S. E. Pearson, Phys. Rev. 132, 2010 (1963).
[16]A. H. M. Kipperman and C. J. Vermij, Nuovo Cimento B LXIII 1, (1969).
[17]C. G. Fonstad and R. H. Rediker, J. Appl. Phys. 42, 2911 (1971).
[18]T. L. Chu, A. Kunioka, and R. W. Kelm, Jr., Solid-State Electron. 14, 1259 (1971).
[19]A. C. Thorsen and H. M. Manasevit, J. Appl. Phys. 42, 2519 (1971).
[20]B. Brückner, Phys. Status Solidi A 4, 685 (1971).